Improvement in Aluminum Complexes Bearing Schiff Base in Ring-Opening Polymerization of ε-Caprolactone: A Five-Membered Ring System

Chieh-Ling Lee,[a] Ya-Fan, Lin,[ae] Man-Ting, Jiang,[a] Wei-Yi Lu,[a] Jaya Kishore Vandavasi,[c] Li-Fang Wang,[a] Yi-Chun Lai,[a] Michael Y. Chiang,[ab] Hsuan-Ying Chen,*[ad]

a Department of Medicinal and Applied Chemistry, Kaohsiung Medical University, Kaohsiung 80708, Taiwan, R.O.C.

b Department of Chemistry, National Chung Hsing University, Taichung 402, Taiwan, R.O.C.

c Department of Chemistry, University of Ottawa, Ontario, Canada

[d] Department of Medical Research, Kaohsiung Medical University Hospital, Kaohsiung 80708, Taiwan, R.O.C.

[e] Department of Fragrance and Cosmetic Science, Kaohsiung Medical University, Kaohsiung 80708, Taiwan, R.O.C.

Electronic supplementary information available: Polymer characterization data, and details of the kinetic study.

Table of Contents

Details of the Kinetic Study of ε-Caprolactone Polymerization

A typical kinetic study was conducted to establish the reaction order with respect to monomer and various Al complexes. For CL polymerization, ε-caprolactone (1.14g, 0.01 mol) was added to a solution of the mixture of Al complexes (0.1 mmol) and BnOH (0.02 mmol) in toluene (5 mL), respectively. The solution was then stirred at room temperature under nitrogen. At the indicated time intervals, 0.05 mL aliquots were removed, trapped with $CDCl_3$ (1mL), and analyzed by ^1H NMR. The ε-caprolactone concentration [CL] was determined by integrating the triplet methylene peak of CL at 4.20 ppm and the triplet methylene peak of polylactone at 4.00 ppm. As expected, plots of $\ln([CL]_0/[CL])$ vs. time for a wide range of Al complexes are linear, indicating the usual first order dependence on monomer concentration (Figures S1-S2, Table S1). Thus, the rate expression can be written as $-d[CL]/dt = k_{obs}[CL]^1$, where $k_{obs} = k_{app}[\text{Al complex} + 2\ \text{BnOH}]^x$. A plot of ($k_{obs}$) vs. [Al complex + 2 BnOH] (Figure S3, Table S2) is linear, indicating the order of [Al complex + 2 BnOH] (x = 1) and k_{app} which is 0.296 $M^{-1}min^{-1}$.

Table S1. The kinetic study of polymerizations of ε-caprolactone using various Al complexes as catalysts

Time/min	$L^{5\text{-}Ph}AlMe_2$	$L^{5\text{-}OMe}AlMe_2$	$L^{5\text{-}Py}AlMe_2$	$L^{5\text{-}OTs}AlMe_2$	$L^{5\text{-}Fu}AlMe_2$	$L^{5\text{-}Thio}AlMe_2$
	Conv of PCL					
10				0.06		
15	0.14					
20	0.18	0.1		0.18		0.04
30	0.255	0.15				0.05
40	0.32					0.06
50				0.46		0.10
60	0.50	0.32	0.10	0.54	0.05	
65						
80				0.69		0.12
90	0.66	0.48	0.22	0.76		
100				0.79	0.10	
110				0.86	0.13	0.16
120	0.76	0.61	0.38	0.9		

140					0.17	0.20
150	0.89	0.70	0.50			
165	0.93					
170					0.19	0.24
180		0.79	0.62			
200						0.29
210			0.66			
230					0.25	
240		0.94	0.74			
290					0.31	0.35
300			0.79			
330			0.83			
350					0.35	0.41
360			0.85			
390			0.87			
450			0.88			
540			0.91			
1280					0.61	
1400						
1460					0.68	0.85
1520					0.71	
1580					0.74	
1640					0.75	
$k_{obs} \times 10^3$	15.79 (92)	9.02 (10)	5.95 (2)	19.52 (130)	1.30 (3)	1.28 (2)
Induction period/min	12 (5)	13 (4)	35 (8)	14 (5)	10 (7)	0
R^2	0.9881	0.974	0.9951	0.9849	0.9963	0.9988

Time/min	$L^{6-Ph}AlMe_2$	$L^{6-Bn}AlMe_2$	$L^{6-OMe}AlMe_2$
	Conv of PCL		
150		0.09	
180	0.32	0.16	
220			0.15
240	0.47		
280			0.34
300	0.58	0.23	
320			0.48
360	0.67		
375		0.32	
380			0.67
410			0.77
420	0.79		
440			0.86
450		0.40	
470			0.90
480	0.87		
500			
540	0.90		
720		0.68	
840		0.78	
1500		0.94	
$k_{obs} \times 10^3$	5.51 (34)	2.07 (60)	8.65 (88)
Induction period/min	129 (23)	147 (27)	227 (37)
R^2	0.9906	0.9741	0.9753

(a) (b)

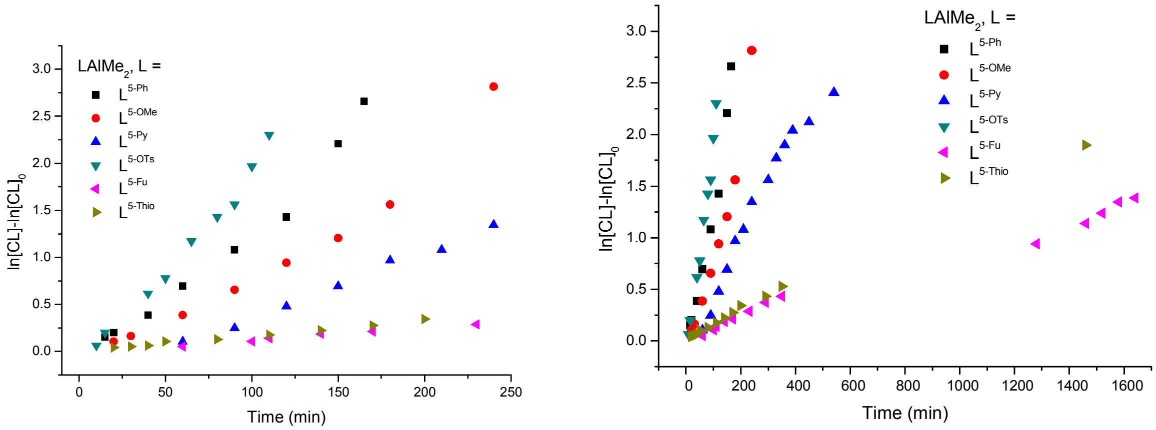

(b)

Figure S1. First-order kinetic plots of ε-caprolactone polymerizations with various 5-membered ring Al complexes plotted against time: (a) Time scale: 0-250 min ; (b) 0-1700 min.

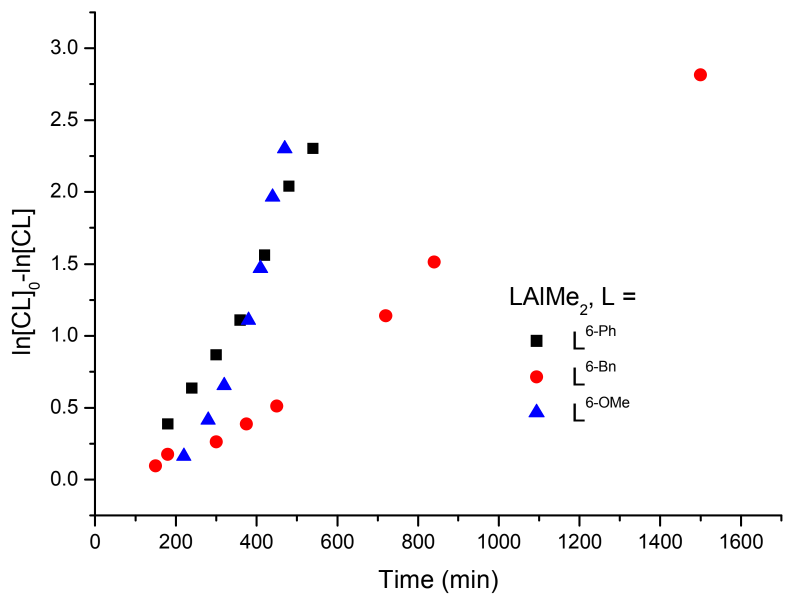

Figure S2. First-order kinetic plots of ε-caprolactone polymerizations with various 6-membered ring Al complexes plotted against time

Table S2. The kinetic study of polymerizations of ε-caprolactone using various concentrations of $\mathbf{L^{5\text{-}OMe}AlMe_2}$ as a catalyst and BnOH as an initiator (average for three experiments)

Time (min)	$[\mathbf{L^{5\text{-}OMe}AlMe_2}$ + 2 BnOH]			
	0.02 M	0.04 M	0.08 M	0.12 M
	PCL conv.			
10			0.14 (4)	0.17 (3)
20		0.10 (2)	0.26 (1)	0.36 (1)
30		0.15 (2)		0.51 (1)
40			0.48 (2)	0.67 (2)
50			0.6 (3)	0.74 (2)
60		0.32 (2)		
65				0.83 (1)
70			0.75 (3)	
90		0.47 (2)		
110			0.83 (2)	
115				0.96 (1)
120		0.60 (3)		
140			0.89 (1)	
150	0.13 (1)	0.70 (1)		
180		0.78 (3)		
210	0.21 (1)			
270	0.23 (1)			
1572	0.56 (2)			
1802	0.63 (3)			
3250	0.79 (2)			
$k_{obs} \times 10^3$	0.45 (2)	8.81 (26)	15.96 (101)	29.05 (41)
Induction period/min	0	13 (3)	0	4 (1)
R^2	0.9976	0.9979	0.9901	0.9995

Table S3. The kinetic study of polymerizations of ε-caprolactone using various concentrations of $\mathbf{L^{5\text{-}OMe}AlMe_2}$ as a catalyst and BnOH as an initiator (test for three times)

Time (min)	$[\mathbf{L^{5\text{-}OMe}AlMe_2} + 2\ \mathrm{BnOH}]$											
	0.02 M			0.04 M			0.08 M			0.12 M		
	PCL conv.											
	1 st	2 nd	3 rd	1 st	2 nd	3 rd	1 st	2 nd	3 rd	1 st	2 nd	3 rd
10							0.1	0.15	0.18	0.15	0.16	0.20
20				0.10	0.11	0.08	0.25	0.27	0.26	0.35	0.37	0.36
30				0.15	0.17	0.13				0.51	0.50	0.52
40							0.46	0.50	0.47	0.66	0.69	0.66
50							0.58	0.63	0.59	0.75	0.72	0.76
60				0.32	0.33	0.30						
65										0.82	0.83	0.83
70							0.73	0.78	0.75			
90				0.48	0.48	0.45						
110							0.81	0.85	0.84			
115										0.96	0.95	0.96
120				0.61	0.62	0.57						
140							0.88	0.90	0.89			
150	0.12	0.13	0.14	0.70	0.70	0.69						
180				0.79	0.80	0.75						
210	0.20	0.22	0.21									
270	0.22	0.24	0.22									
1572	0.55	0.58	0.56									
1802	0.60	0.66	0.62									
3250	0.78	0.81	0.79									
$k_{obs} \times 10^3$	0.43 (1)	0.48 (2)	0.45 (1)	9.02 (10)	9.12 (10)	8.31 (23)	15.36 (96)	16.77 (128)	16.04 (96)	29.13 (50)	26.96 (99)	28.87 (52)
Induction period/min	0	0	0	13 (4)	12 (5)	14 (3)	0	0	0	4 (1)	2 (2)	3 (1)

R^2	0.9987	0.996	0.998	0.974	0.976	0.998	0.9903	0.9859	0.9911	0.9993	0.9967	0.9992

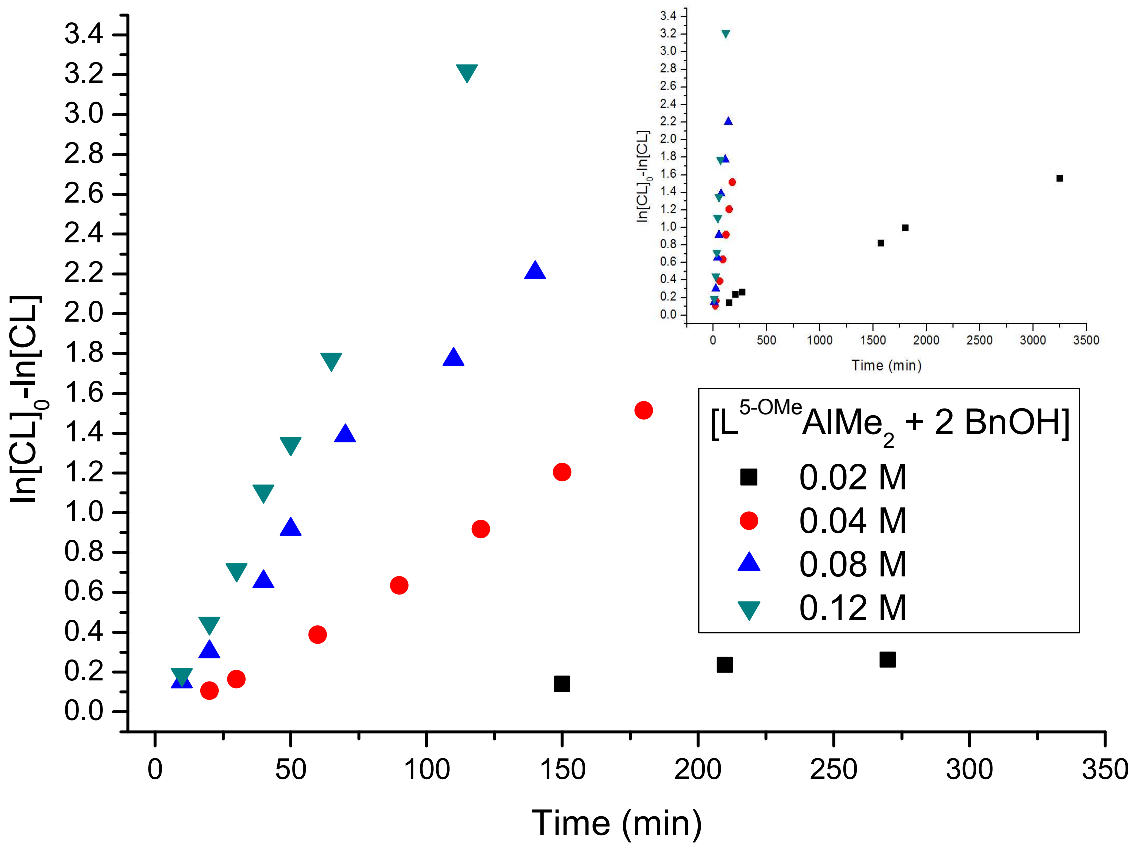

Figure S3. First-order kinetic plots of CL polymerization with various concentrations of [$\mathbf{L^{5\text{-}OMe}AlMe_2}$ + 2 BnOH] plotted against time with [CL] = 2.0 M in toluene 5 mL (the first test of **Table S2**).

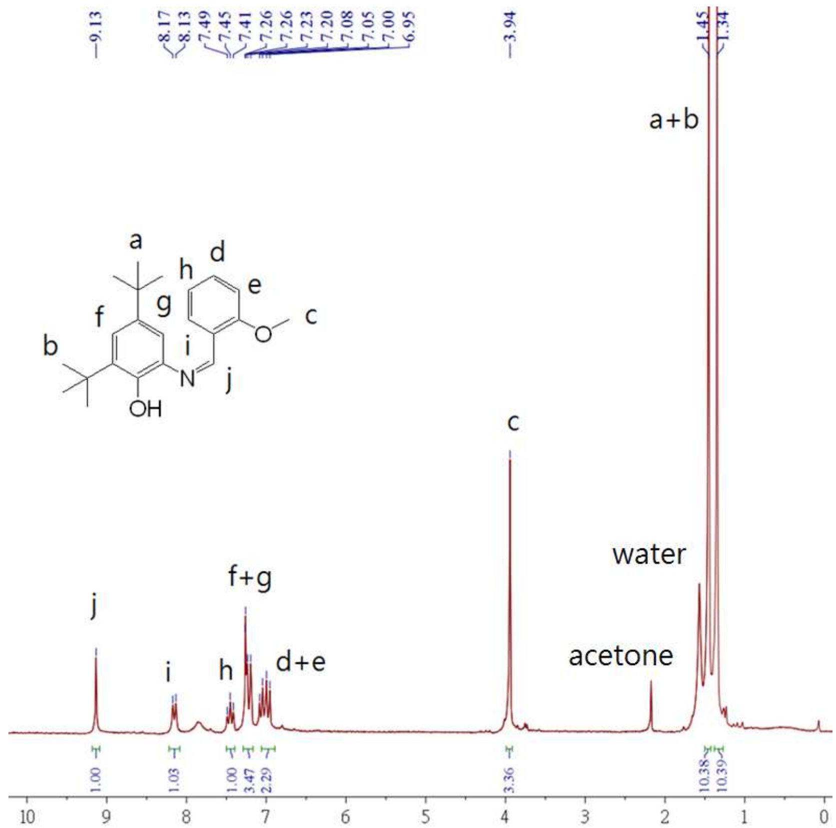

Figure S4. ^{1}H NMR spectrum of $\mathbf{L^{5\text{-}OMe}\text{-}H}$ in $CDCl_3$

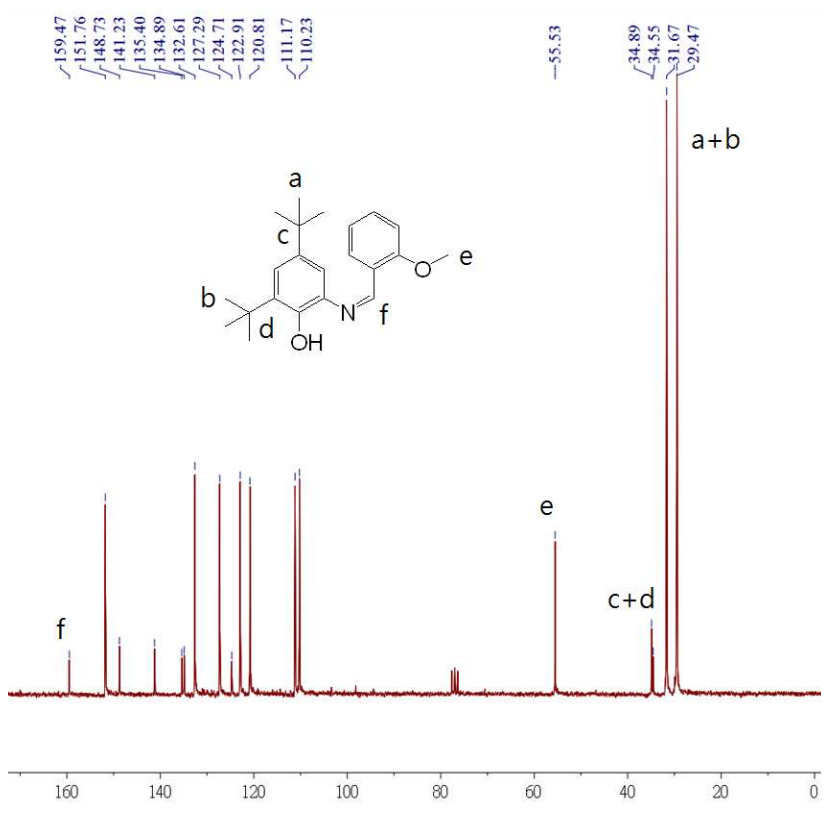

Figure S5. ^{13}C NMR spectrum of $\mathbf{L^{5\text{-}OMe}\text{-}H}$ in $CDCl_3$

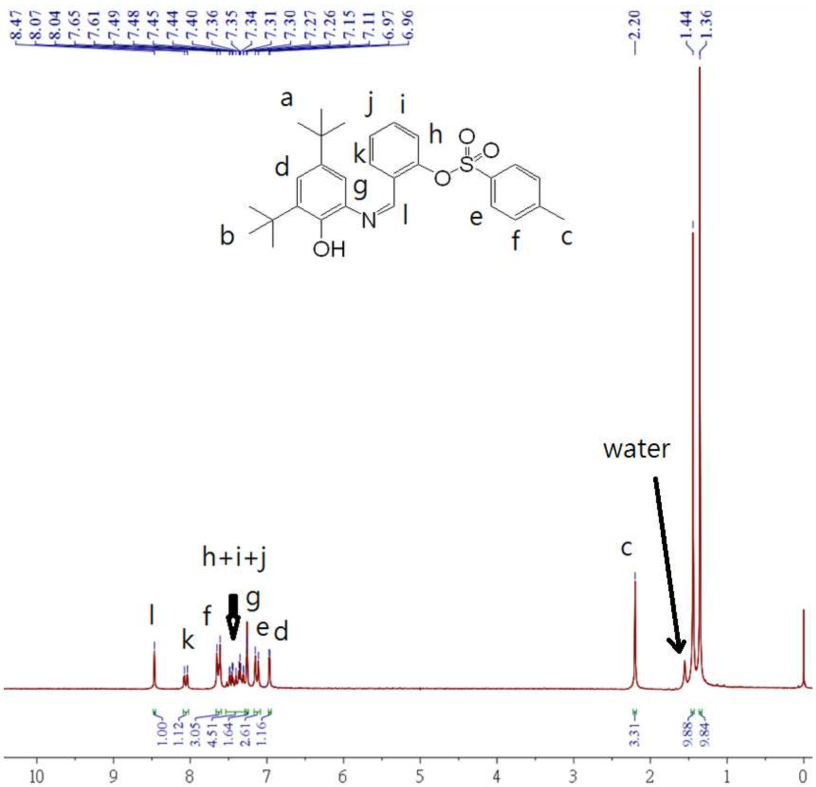

Figure S6. ^{1}H NMR spectrum of $\mathbf{L^{5\text{-}OTs}\text{-}H}$ in $CDCl_3$

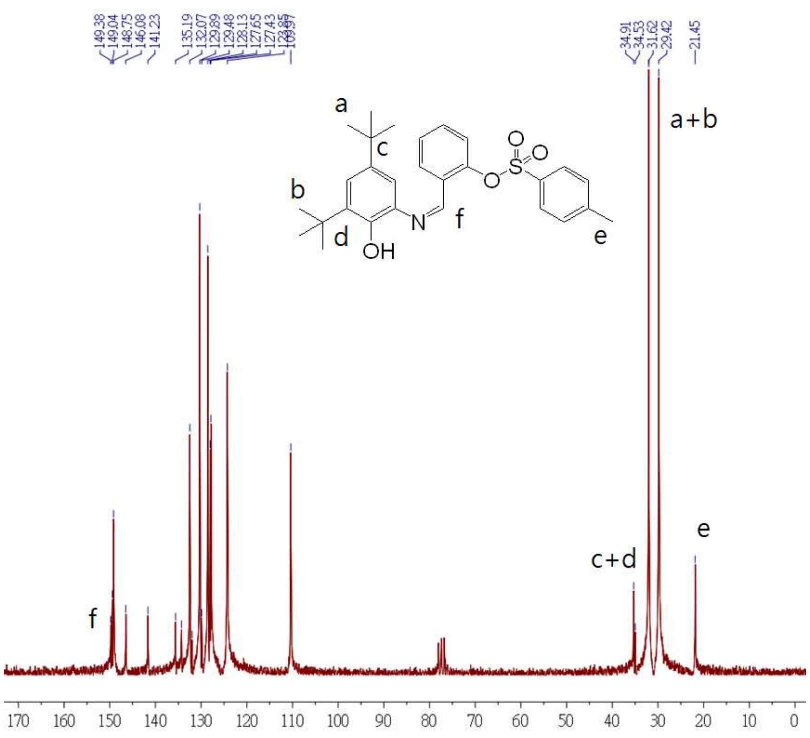

Figure S7. ^{13}C NMR spectrum of $\mathbf{L^{5\text{-}OTs}\text{-}H}$ in $CDCl_3$

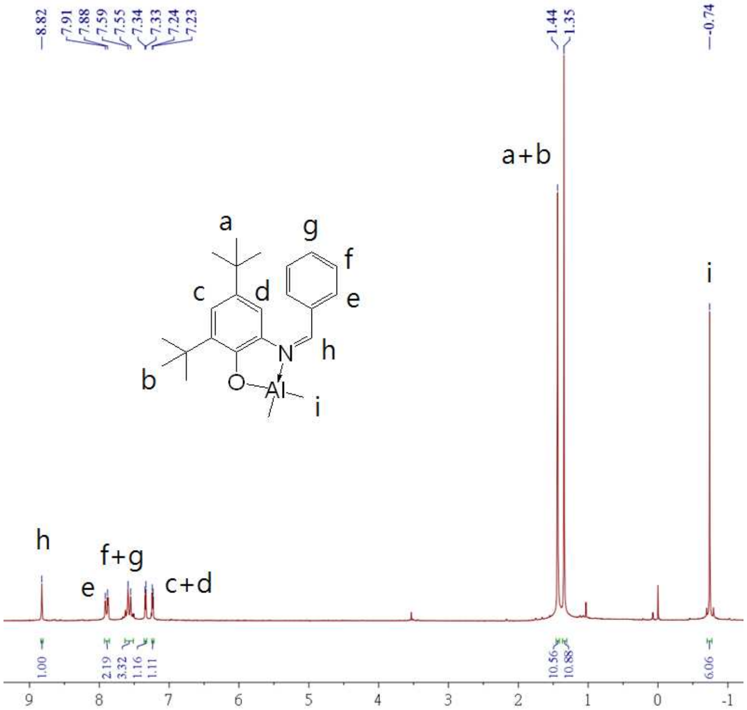

Figure S8. ^{1}H NMR spectrum of **L$^{5\text{-}Ph}$AlMe$_2$** in $CDCl_3$

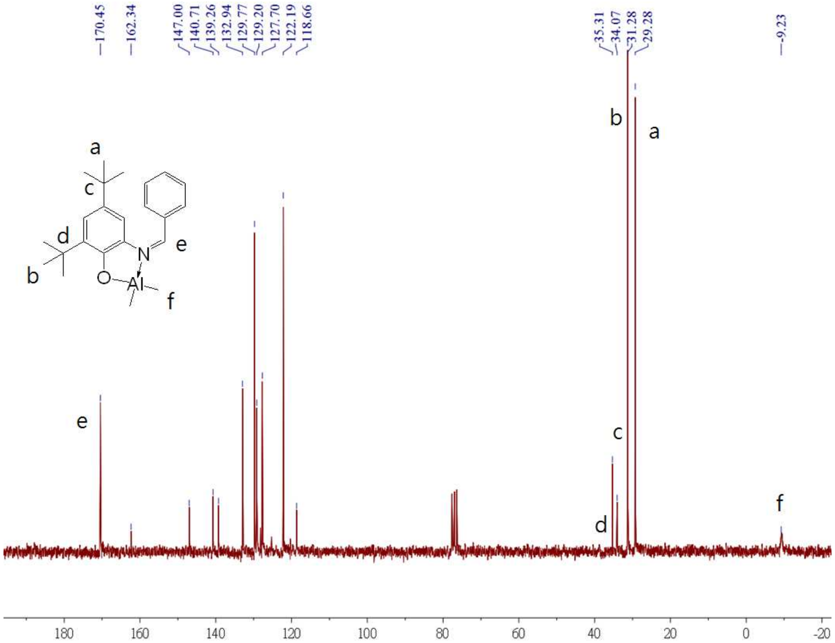

Figure S9. ^{13}C NMR spectrum of **L$^{5\text{-}Ph}$-AlMe$_2$** in $CDCl_3$

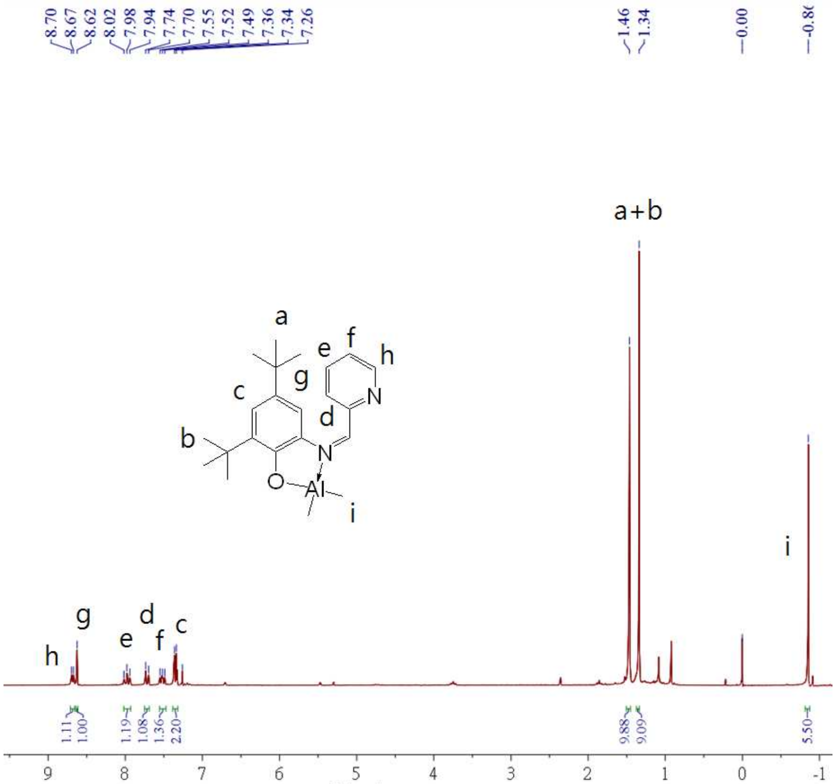

Figure S10. ^{1}H NMR spectrum of $\mathbf{L^{5\text{-}Py}AlMe_2}$ in $CDCl_3$

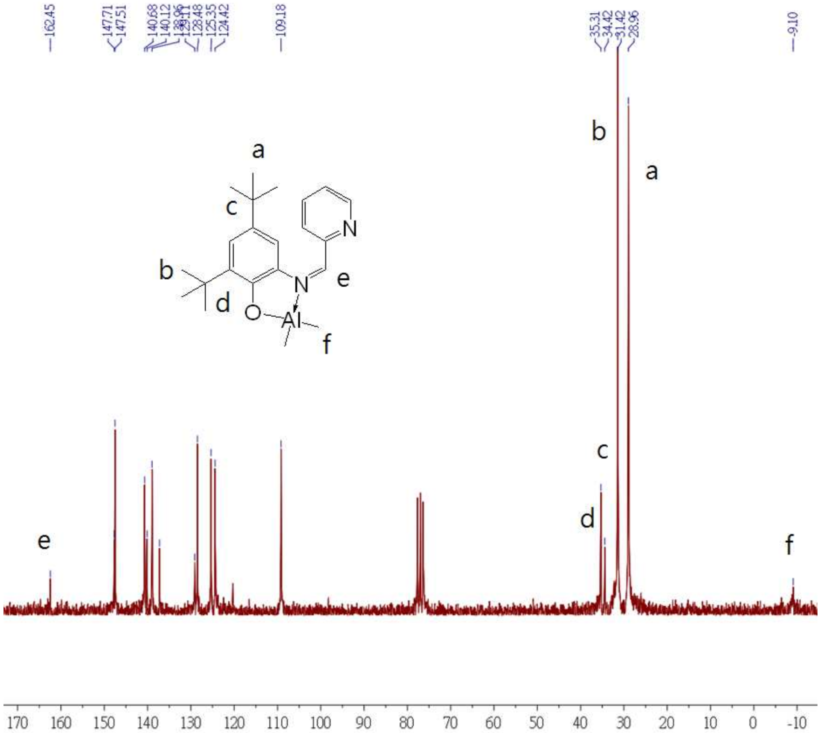

Figure S11. ^{13}C NMR spectrum of $\mathbf{L^{5\text{-}Py}AlMe_2}$ in $CDCl_3$

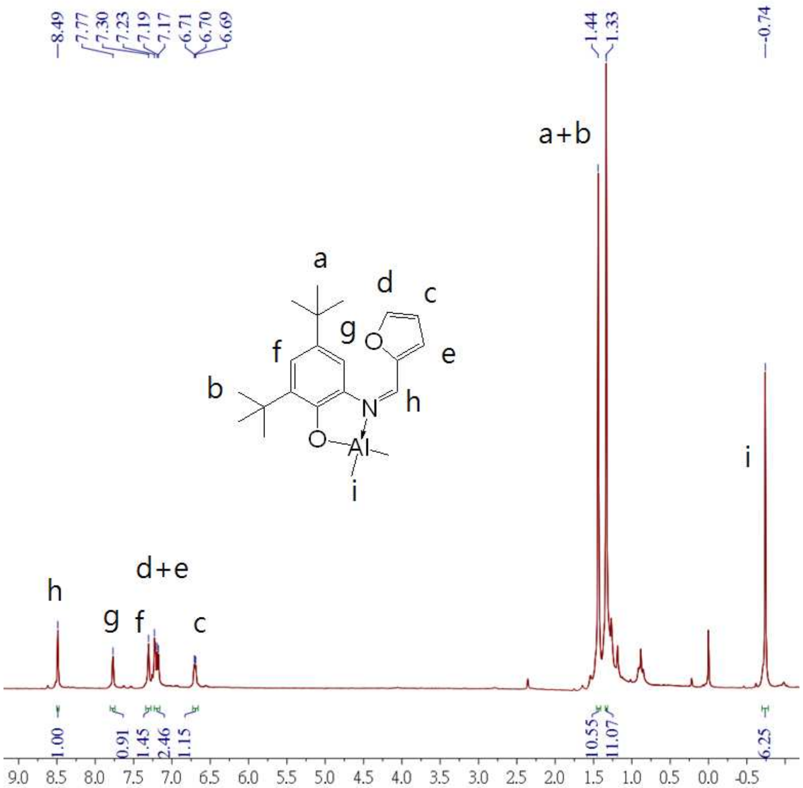

Figure S12. ^{1}H NMR spectrum of $\mathbf{L^{5\text{-}Ful}AlMe_2}$ in $CDCl_3$

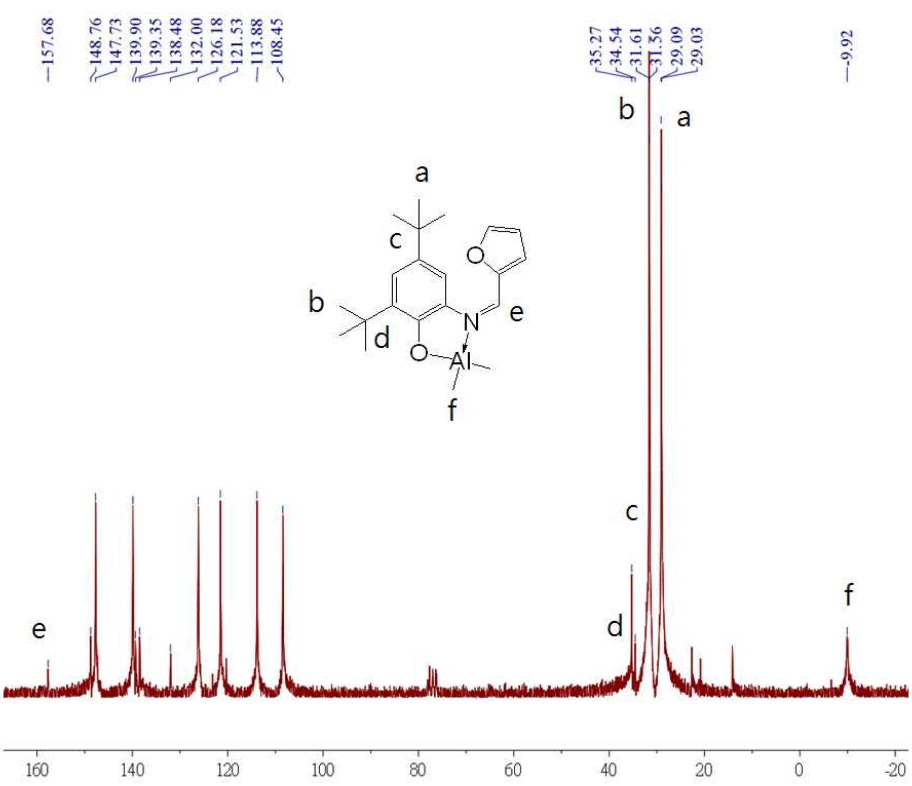

Figure S13. ^{13}C NMR spectrum of $\mathbf{L^{5\text{-}Ful}AlMe_2}$ in $CDCl_3$

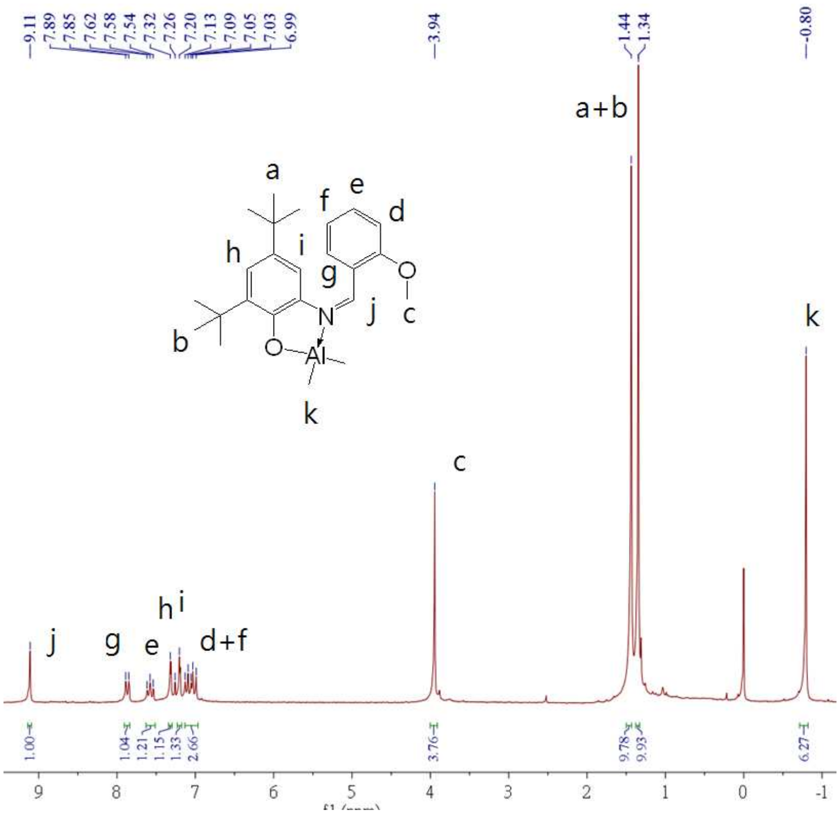

Figure S14. ^{1}H NMR spectrum of **L$^{\mathbf{5\text{-}OMe}}$AlMe$_2$** in $CDCl_3$

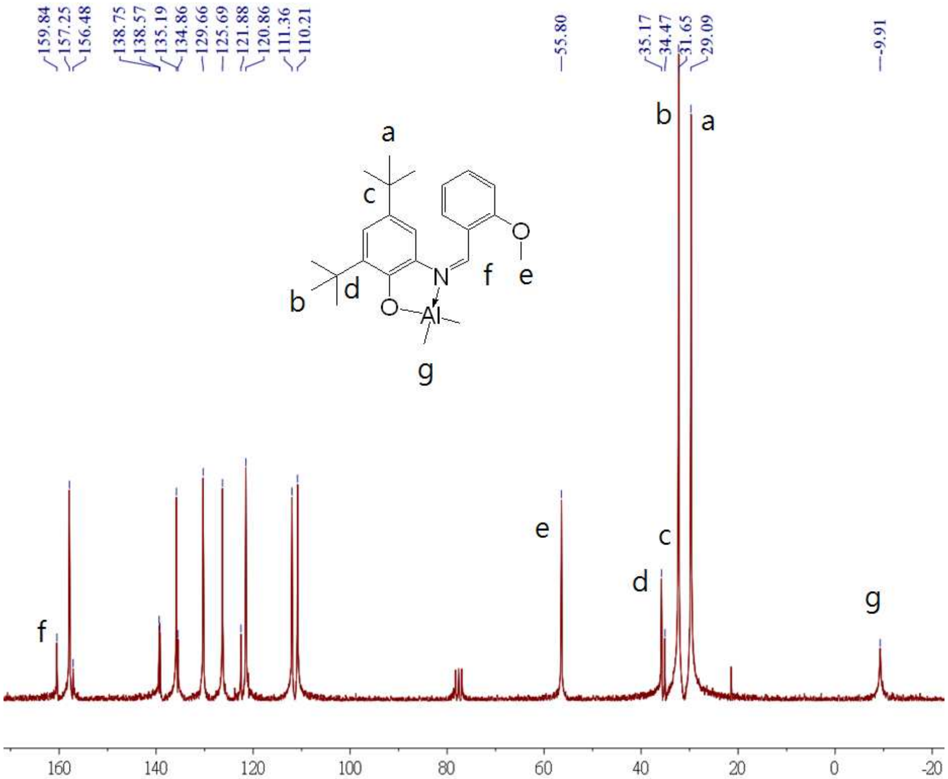

Figure S15. ^{13}C NMR spectrum of **L$^{\mathbf{5\text{-}OMe}}$AlMe$_2$** in $CDCl_3$

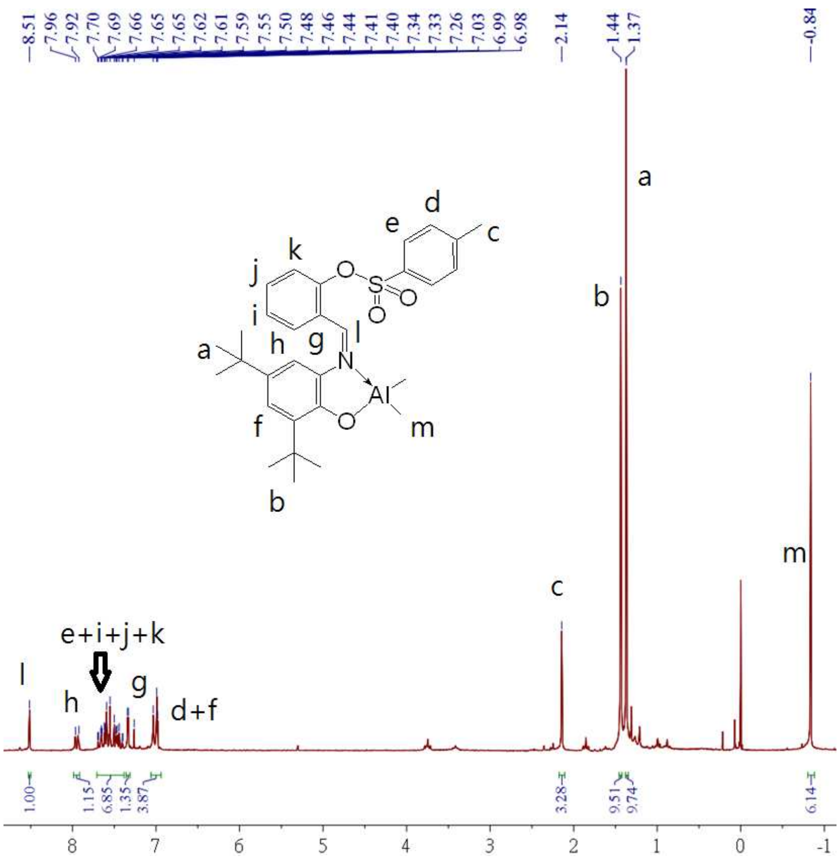

Figure S16. ^{1}H NMR spectrum of $\mathbf{L^{5\text{-}OTs}AlMe_2}$ in $CDCl_3$

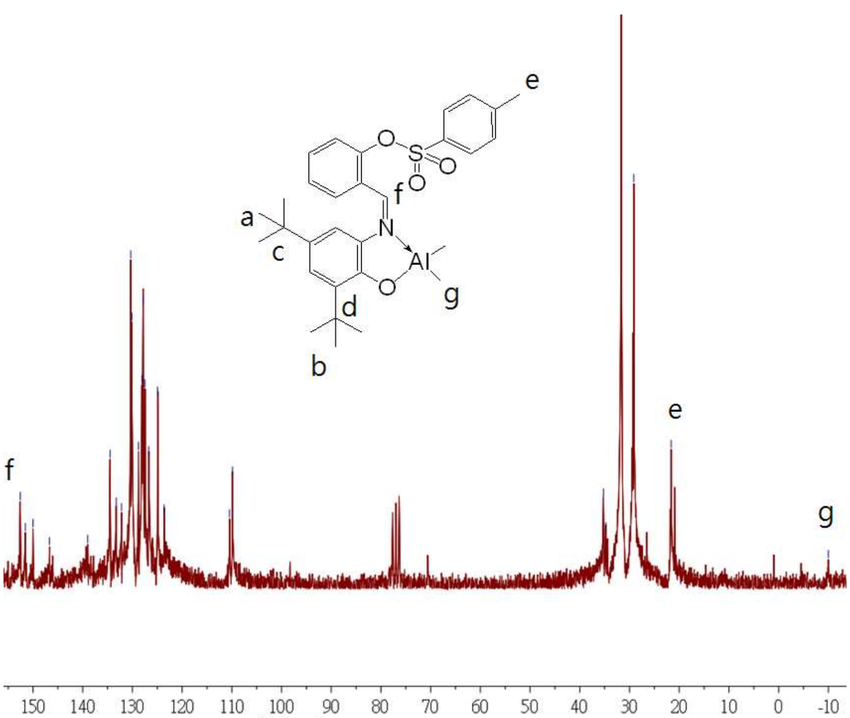

Figure S17. ^{13}C NMR spectrum of $\mathbf{L^{5\text{-}OTs}AlMe_2}$ in $CDCl_3$

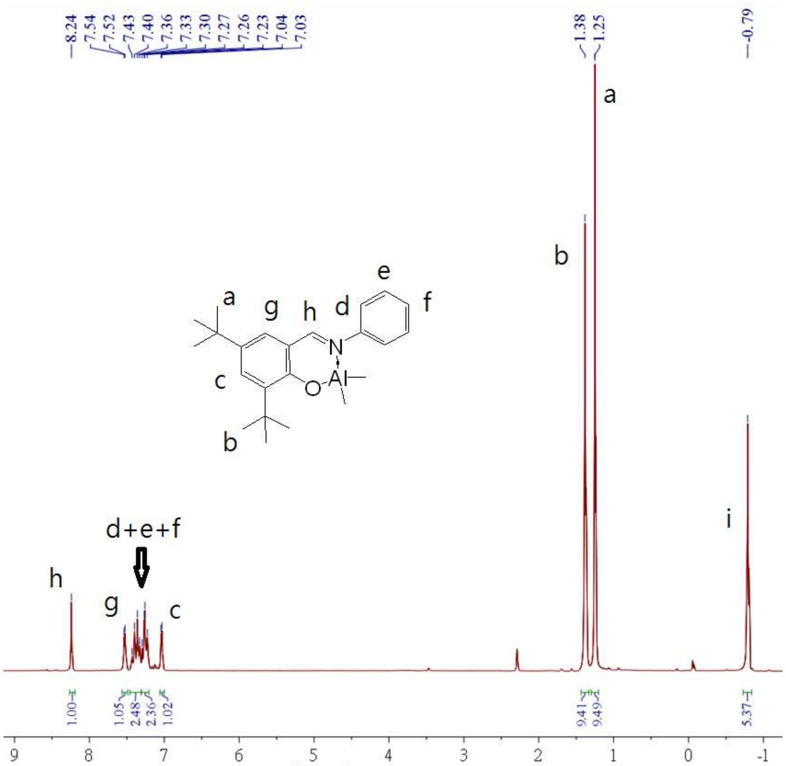

Figure S18. ^{1}H NMR spectrum of $\mathbf{L^{6\text{-}Ph}AlMe_2}$ in $CDCl_3$

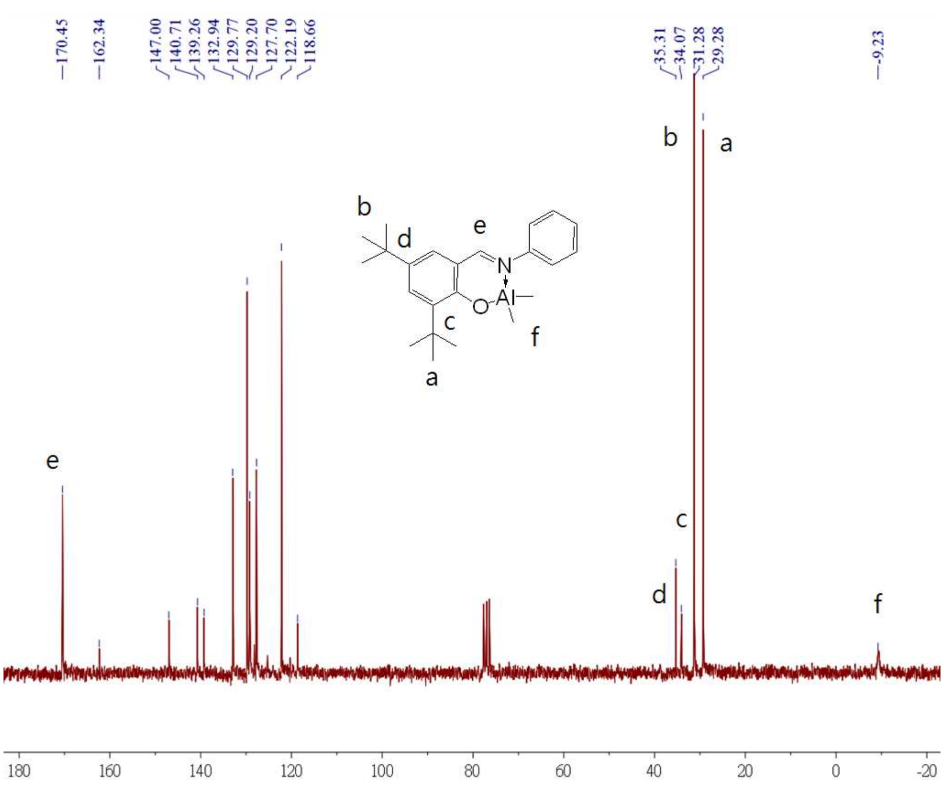

Figure S19. ^{13}C NMR spectrum of $\mathbf{L^{6\text{-}Ph}AlMe_2}$ in $CDCl_3$

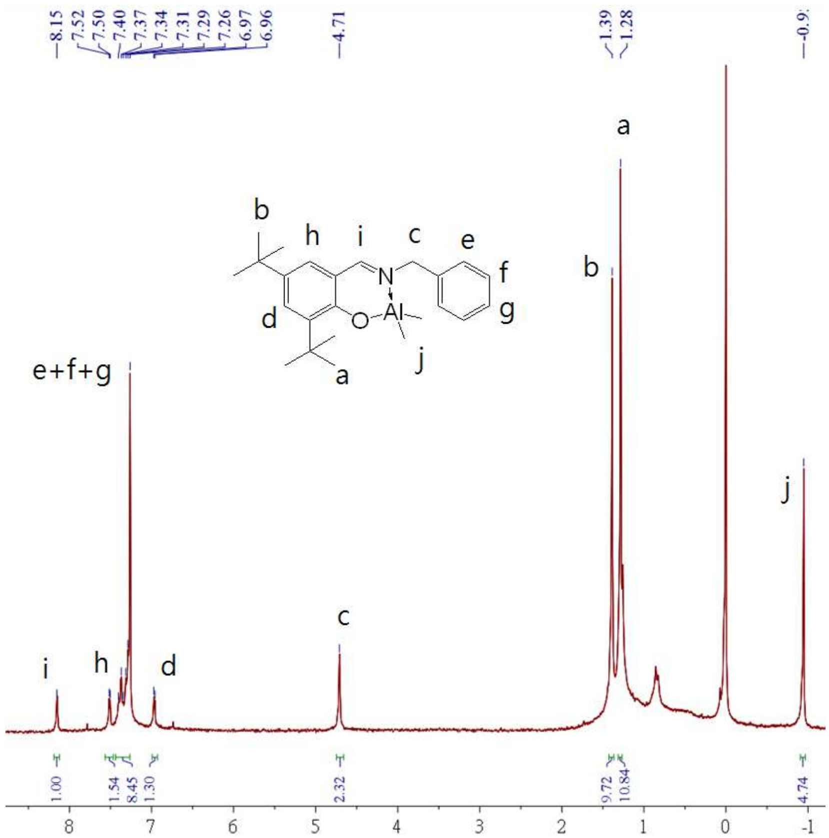

Figure S20. ^{1}H NMR spectrum of $\mathbf{L^{6\text{-}Bn}AlMe_2}$ in $CDCl_3$

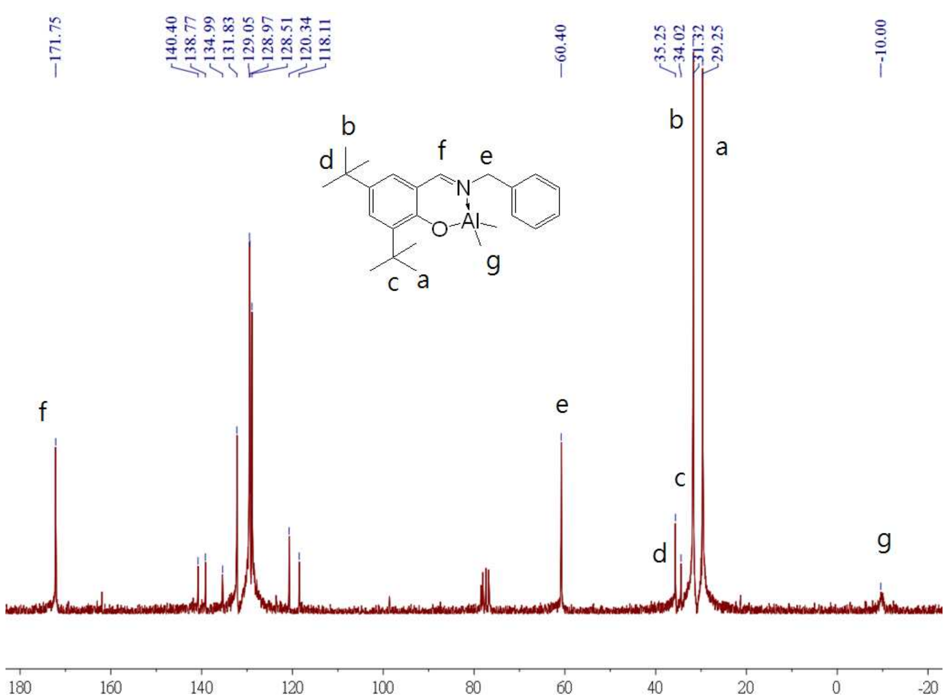

Figure S21. ^{13}C NMR spectrum of $\mathbf{L^{6\text{-}Bn}AlMe_2}$ in $CDCl_3$

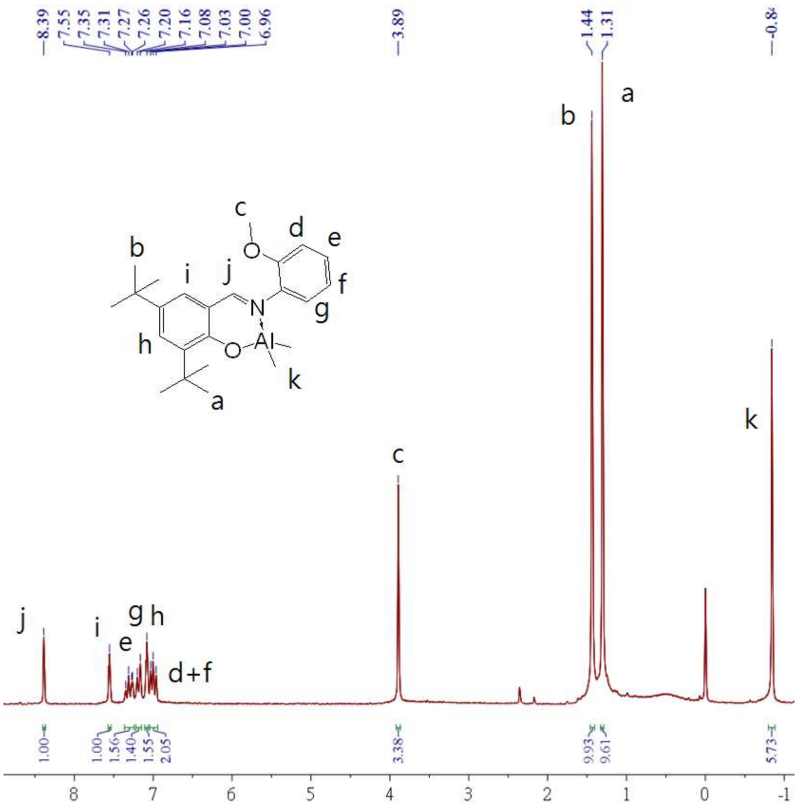

Figure S22. ^{1}H NMR spectrum of $\mathbf{L^{6\text{-}OMe}AlMe_2}$ in $CDCl_3$

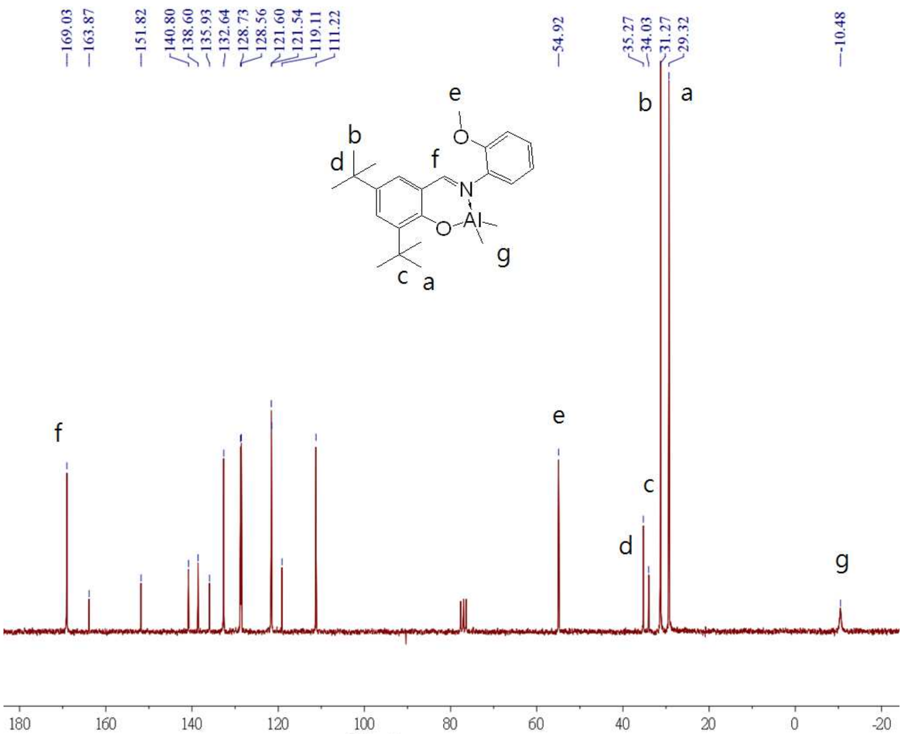

Figure S23. ^{13}C NMR spectrum of $\mathbf{L^{6\text{-}OMe}AlMe_2}$ in $CDCl_3$

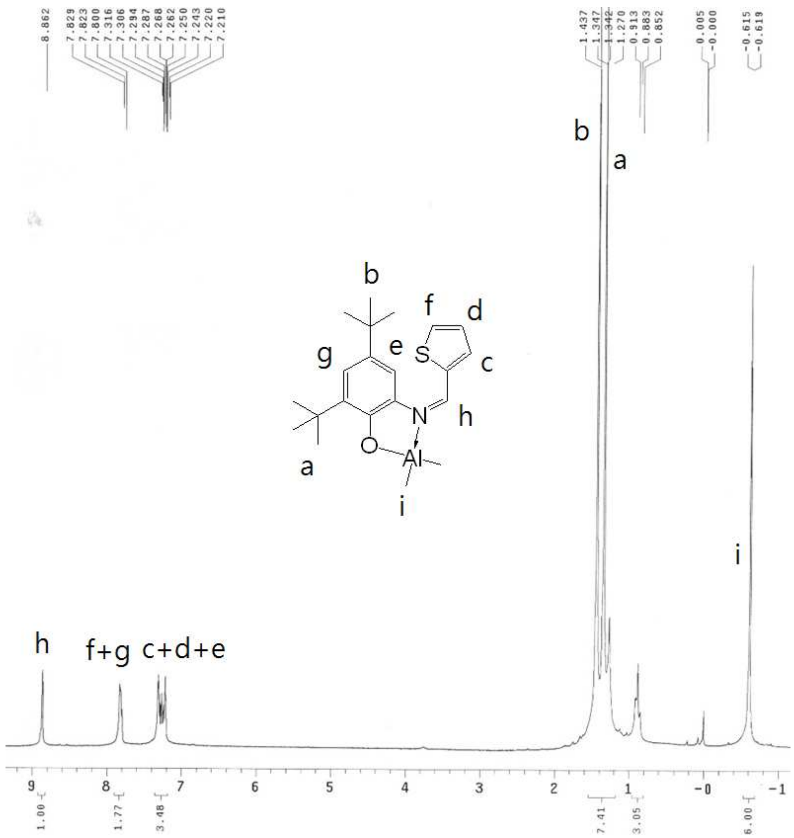

Figure S24. ^{1}H NMR spectrum of $\mathbf{L^{5\text{-}Thio}AlMe_2}$ in $CDCl_3$

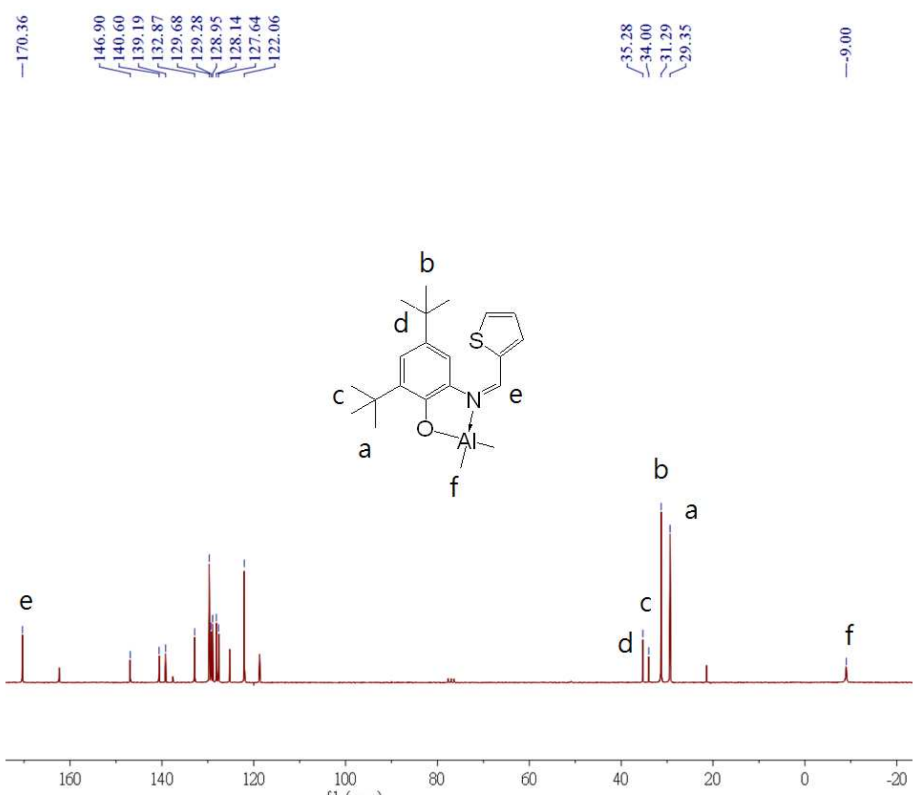

Figure S25. ^{13}C NMR spectrum of $\mathbf{L^{5\text{-}Thio}AlMe_2}$ in $CDCl_3$

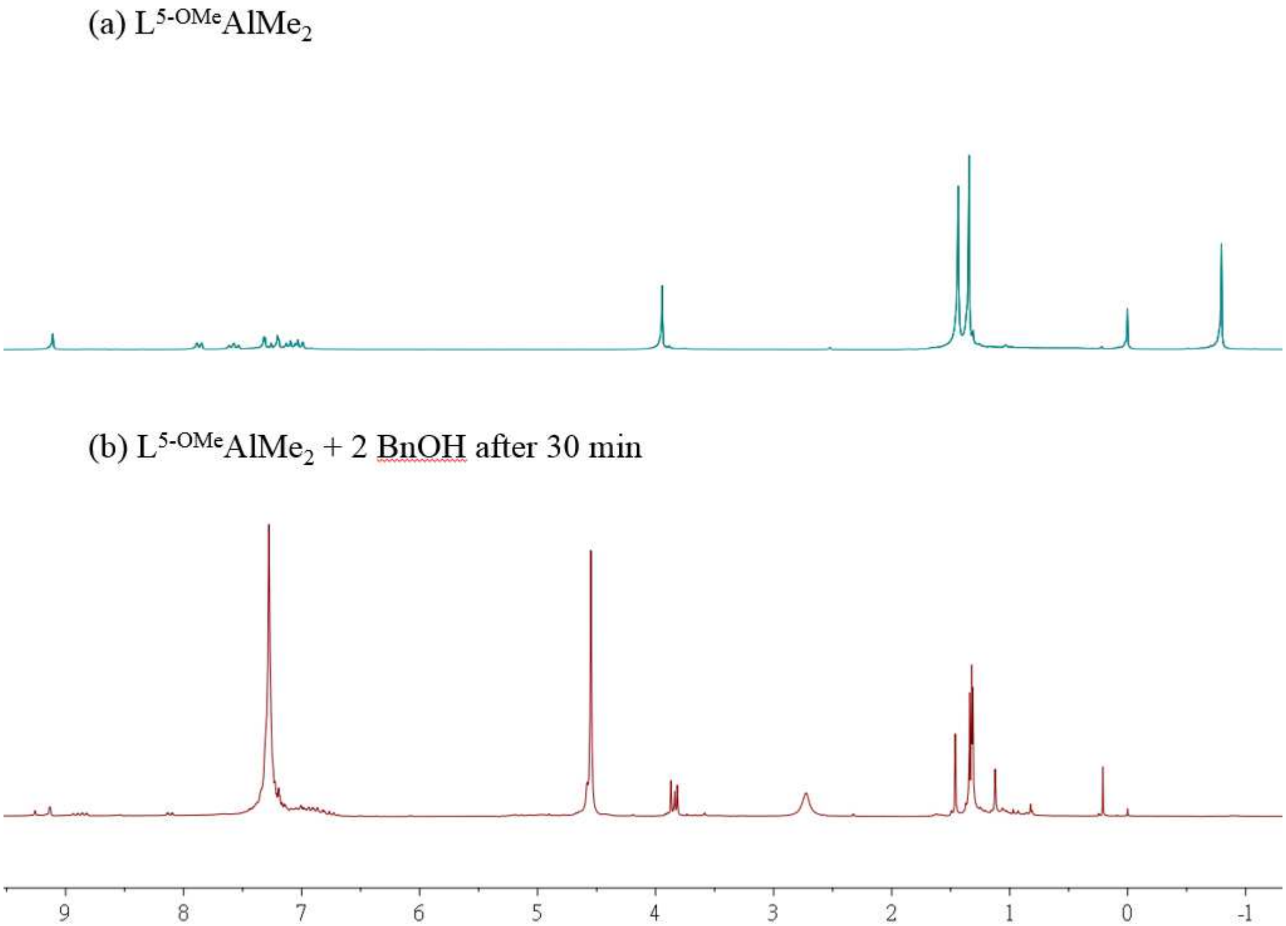

Figure S26. ^{1}H NMR spectrum of (a) $\mathbf{L^{5\text{-}OMe}AlMe_2}$ and (b) the reaction of $\mathbf{L^{5\text{-}OMe}AlMe_2}$ and BnOH (1:2) after 30 min.

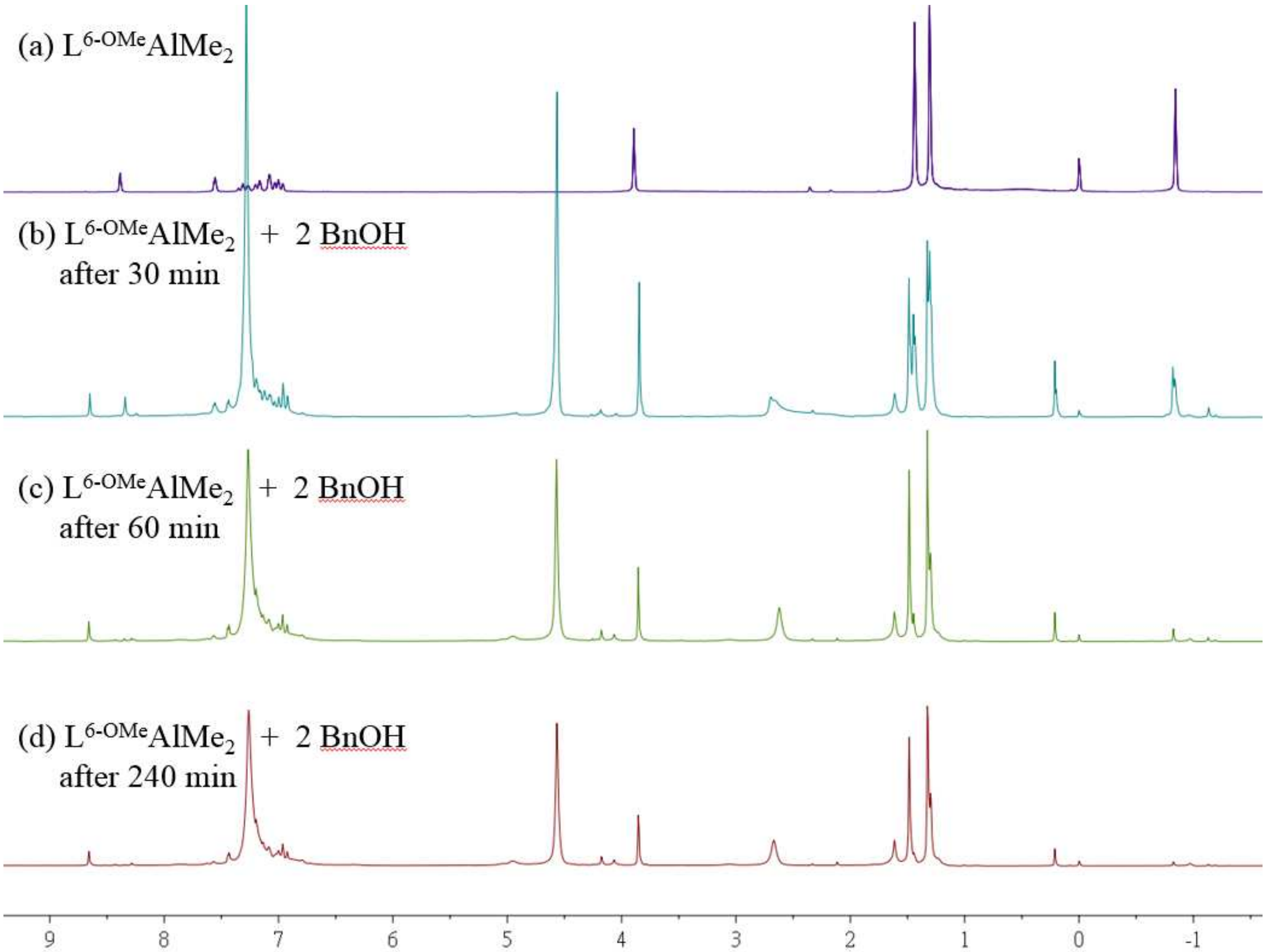

Figure S27. ^{1}H NMR spectrum of (a) **L$^{6\text{-}OMe}$AlMe$_2$**, (b) the reaction of **L$^{6\text{-}OMe}$AlMe$_2$** and BnOH (1:2) after 30 min, (c) 60 min, and (d) 240 min.